Calculation of Transonic Potential Flowfields About Complex, Three-Dimensional Configurations*

D. A. Caughey** and Antony Jameson***

ABSTRACT

Methods for extending iterative, finite-difference calculations of transonic potential flowfields to complex three-dimensional configurations are discussed. One particularly attractive approach is to use relatively simple conformal mappings in combination with shearing transformations to generate computational domains that are nearly-conformally mapped from the physical space in one family of coordinate surfaces, and which map the complex boundaries to grid surfaces. The application of such a method to a general wing-body combination or to a multibladed fan is discussed. A transformation to map the wing-fuselage or fan-hub combination to a convenient computational domain is proposed. The transformation is useful in its own right for treating the two-dimensional problems of flow past a profile in a wind tunnel or through a cascade. Some results of preliminary calculations are presented.

---

*This work was supported by NASA under Grants NGR 33-016-167 and NGR 33-016-201. The computations were performed at the ERDA Mathematics and Computing Laboratory, New York University, under Contract E(11-1)-3077.

**Assistant Professor, Sibley School of Mechanical and Aerospace Engineering, Cornell University, Ithaca, New York.

***Professor, Courant Institute of Mathematical Sciences, New York University, New York, New York.

INTRODUCTION

In recent years, iterative solutions of finite-difference approximations to the transonic potential equation have met with remarkable success. These methods have been used to predict the inviscid, mixed flowfields about airfoils[1], wings[2], and simple wing-body combinations[3] within the framework of small-disturbance theory; they have also been applied to calculate the inviscid, transonic flowfields about airfoils[4,5], bodies of revolution[5,6], nacelles[7,8], and oblique[9] and swept[10] wings using the full potential equation.

There are two computational advantages of using small-disturbance theory. First, the equation is somewhat simpler,and its type is completely determined by the coefficient of the ϕ_{xx} term, allowing the construction of relatively simple type-dependent differencing schemes. Second, the boundary conditions can usually be transferred to some mean surface which can often be chosen as a coordinate plane in a simple cartesian system. For complex geometries, this is a great simplification, since the treatment of boundary conditions in cases when the boundary surface does not coincide with grid points is generally either very complicated and time-consuming or inaccurate.

When using the full potential equation the use of such mean surface approximations is generally inconsistent with the accuracy of the equation itself. The alternatives are (1) to use interpolation formulas to apply the boundary conditions at the grid points nearest the boundary surfaces, or (2) to use coordinate transformations which reduce the boundaries to coordinate surfaces. At the present time it is not clear which approach is better for the handling of complex geometrical shapes. The interpolation schemes require additional complexity in the difference codes to treat the variety of mesh-boundary intersections that may occur; the transformation method adds

complexity to the equations themselves, and may require additional storage for transformation derivatives. Our approach is the latter. In this case the boundary conditions are satisfied exactly (in a finite-difference sense) on the boundary surfaces; it is also hoped that since the transformations need be calculated only once at the beginning of the solution, the method will compare favorably in terms of speed with the grid-interpolation methods.

PROPOSED ANALYSIS

Conformal transformations have proved a useful tool for the finite-difference calculation of two dimensional flowfields. A preliminary transformation is performed which maps the body boundary onto some canonical curve (e.g., a profile onto the unit circle), and a finite-difference grid is set up in convenient coordinates in the mapped plane for which the canonical curve is a coordinate line. A difference approximation to the transformed equation is then solved by relaxation, with the boundary conditions applied along the appropriate coordinate lines.

Much of the advantage of this approach is lost when we go to problems in three dimensions, because there is no generalization of conformal mapping in this case. Also, if we perform separate conformal mappings to canonical curves in each of some family of coordinate surfaces, we lose orthogonality, so that numerous mapping derivatives have to be calculated. The labor of determining the map functions at each point of the grid, and the storage required to save them for repeated use during the iterative solution of the difference equations, can then become excessive.

An attractive alternative approach has been used by Jameson for calculating the three-dimensional flow past yawed[9] and swept[10] wings. The same basic idea has been applied to the flow past axisymmetric inlet nacelles by Caughey and Jameson[7]. The method consists of applying a simple conformal transformation (which can usually be generated by elementary functions) in each of one family of coordinate surfaces which <u>almost</u> maps the boundary surfaces to coordinate planes. A shearing transformation is then introduced to complete the mapping of the boundaries to coordinate surfaces. This final transformation renders

the coordinate system non-orthogonal, but if the initial conformal mapping is carefully chosen, the shearing is everywhere slight, and the weak non-orthogonality seems not to cause any stability problems.

For the analysis of flow past an isolated, three-dimensional wing, a convenient mapping is the square root transformation applied in planes containing the wing section. If the branch point of the transformation is located just inside the leading edge of the profile at each spanwise station, this has the effect of mapping the wing surface to a shallow bump, which can then be reduced to a plane by a simple shearing transformation. The square-root transformation is particularly nice because the mapping modulus and its derivatives can all be calculated from the coordinates in the mapped plane using only algebraic (non-transcendental) functions. Thus, there is little to be gained by storing the mapping derivatives; rather they can be rapidly calculated each time they are needed. The result of a typical calculation using this method is presented in Figure 1.

To treat more complex configurations in a similar manner, we need to reduce all boundary surfaces to shallow bumps by simple mappings. An example of the next level of complexity we have in mind is shown in Figure 2. We consider a wing mounted on a fuselage having a circular cross-section of varying radius denoted by $R(x)$. We assume the flow is symmetric about the vertical plane containing the fuselage centerline, so that we may apply a symmetry condition there and consider the flow only in the half space.

We first define a singular line, just inside the leading edge of the wing, which will later be used as the branch point in a conformal map to "unwrap" the wing surface. The location of this singular line can be denoted as

$$x = x_s(z) \ ,$$

$$y = y_s(z) \ ,$$

where x_s', y_s' will correspond to the local sweep and dihedral, respectively, of the singular line. If we then introduce the coordinates

$$\bar{x} = x - x_s(z) ,$$

$$\bar{y} = y - y_s(z) ,$$

and finally

$$r = \sqrt{\bar{y}^2 + z^2}\,/R(x)$$

$$\theta = \tan^{-1}(\bar{y}/z) ,$$

the geometry will be transformed to that shown in Figure 3. A surface of r = constant will then look like Figure 4. It is in these surfaces, then, that we wish to introduce our nearly-conformal transformations. Note that the geometry of Figure 4 corresponds in the two-dimensional case to the flow past a profile in a solid-walled wind tunnel or, if the symmetry conditions at $\theta = \pm \pi/2$ are replaced by periodicity conditions, to the flow past one blade in an infinite, two-dimensional cascade.

The transformation which is the generalization of Jameson's square-root mapping to this case can be shown to be (after a rescaling of θ and a shift in the origin)

$$\bar{x} + i\theta = \log \{1. - \cosh \zeta\} , \qquad (1)$$

where $\zeta = \xi + i\eta$. A schematic representation of the ζ-plane is shown in Figure 5a. The upper and lower symmetry lines (tunnel walls) map to the negative and positive real axes, respectively. The profile maps to a slight bump, near the line $\eta = \pi$. If we let $S(\xi)$ be the width of the infinite strip in the ζ-plane, then the final shearing transformation

$$X = \xi$$

$$Y = \eta/S(X)$$

reduces the strip to one of constant width, as shown in Figure 5b.

A complete sketch of the three-dimensional coordinate system is shown in Figure 6. The space is infinite in the directions of $\pm X$, r, but the computational domain can be rendered a finite rectangular parallelepiped by suitable stretching transformations in these directions.

Finally, it can be mentioned that the above-described coordinate system is a logical one to use for the problem of flow through a fan (or propeller) or a three-dimensional cascade. Figure 7 shows the type of geometry that might be treated in this way. In this case the range of θ treated would be limited to the interval $[-2\pi/N, 2\pi/N]$, where N is the number of fan (or cascade) blades, and the symmetry condition applied on these planes would be replaced by the requirement of periodicity.

A fundamental difference between this problem and that of the wing-fuselage combination is that the onflow would now be rotational in the reference frame rotating with the blades. For cases in which the onflow is irrotational in an absolute frame, however, a reduced potential can be introduced to describe the velocity field in terms of the gradient of a single scalar potential plus a constant rotational component. (See, e.g., Vavra[11].)

PRELIMINARY RESULTS

To demonstrate the efficacy of the coordinate system just described for the calculation of three-dimensional flows, some preliminary two-dimensional calculations have been performed using the mapping of Eq. (1). These particular calculations have been performed using the symmetry condition on the lines $\theta = \pm \pi/2$, and hence correspond to the flow past a profile in a non-ventilated, or solid-wall wind tunnel.

A sketch of the finite-difference mesh produced by this transformation is shown in Figure 8. The sketch shows the point distribution for a very crude grid containing 32 x 8 mesh cells, and is for the geometry of the original Korn airfoil[4] in a tunnel having a total height six times the airfoil chord.

To avoid difficulties at infinity, the singular part of the velocity potential is removed, and the calculation is performed in terms of the reduced potential

$$G = \phi - \overline{X} \ ,$$

where, from Eq. (1),

$$\overline{X} = \log(\cosh \xi - \cos \eta).$$

If we define $T = 1/S(\xi)$,

and

$$U = \phi_\xi = \frac{\sinh \xi}{\cosh \xi - \cos \eta} + G_X + Y_\xi G_Y \ ,$$

$$V = \phi_\eta = \frac{\sin \eta}{\cosh \xi - \cos \eta} + T\, G_Y \ ,$$

the planar potential equation becomes

$$AG_{XX} + BG_{XY} + CG_{YY} + DG_Y + E = 0 \ , \qquad (2)$$

with

$$A = a^2 - U^2/h^2 ,$$

$$B = -2\left\{\frac{U(TV + Y_\xi U)}{h^2} - Y_\xi a^2\right\} ,$$

$$C = a^2(T^2 + Y_\xi{}^2) - \frac{(TV + Y_\xi U)^2}{h^2} ,$$

$$D = (a^2 - U^2/h^2)\eta\, T'' - 2T' \frac{UV}{h^2} ,$$

$$E = \frac{-U^2 + V^2}{h^2} \frac{1 - \cosh\xi \cos\eta}{(\cosh\xi - \cos\eta)^2} + 2\frac{UV}{h^2} \frac{\sinh\xi \sin\eta}{(\cosh\xi - \cos\eta)^2}$$

$$\frac{-(U^2 + V^2)}{h^4} \frac{U \sinh\xi\cos\eta + V\cosh\xi\sin\eta}{(\cosh\xi - \cos\eta)^2} ,$$

where a is the local speed of sound, and h^2 is the square of the modulus of the map function

$$h^2 = \left|\frac{d(\bar{x} + i\theta)}{d(\xi + i\eta)}\right|^2 = \frac{\cosh\xi + \cos\eta}{\cosh\xi - \cos\eta} .$$

The profile shape downstream of the trailing edge is continued smoothly to infinity in the computational domain, and allowance is made for a constant jump in potential across this cut in the physical plane. The magnitude of this jump is determined by the Kutta condition at the trailing edge of the profile.

A finite-difference form of Eq. (2) is solved using the rotated differencing scheme first suggested by Jameson[9]. The equation is solved subject to the conditions that

$$G_Y = \frac{S' \left\{ \frac{\sinh \xi}{\cosh \xi - \cos \eta} + G_X \right\} - \frac{\sin \eta}{\cosh \xi - \cos \eta}}{T(1 + S'^2)}$$

on the profile surface,

$$G_Y = 0$$

on the symmetry lines, and

$$G_X = 0$$

at downstream infinity. The problem for G is thus a purely Neumann one, and the value of G is allowed to float to an arbitrary level during the course of the iteration.

A comparison of two such solutions is shown in Figure 9. The results are for the flow at $M_\infty = 0.75$ past the Korn airfoil at zero angle of attack, and are calculated on a grid containing 128 x 32 mesh cells in the X and Y directions, respectively. One calculation is for the profile in a tunnel having a total height six times the airfoil chord; the other in a tunnel having a total height four times the airfoil chord.

A REMARK ON TWO-DIMENSIONAL CASCADE CALCULATIONS

While the basic mapping of Eq. (1) can be used to perform two-dimensional cascade or wind-tunnel calculations as demonstrated in the preceding section, it is not necessarily the best coordinate system for these problems. For the numerical calculation of flows past isolated profiles, the most accurate results to date have been performed in coordinate systems which conformally map the exterior of the profile to the interior of the unit circle[4,5], as mentioned in the introduction. This has the advantage of allowing a large number of grid points to be placed on the airfoil surface, and of easily allowing concentrations of the points at both the leading and trailing edges of the profile (the latter being especially important for aft-cambered airfoils which have large gradients there).

The analogous mapping for the cascade problem would be to map the physical geometry to a ring. One possible mapping to perform this transformation can be visualized in two steps as shown in Figure 10. First we map the infinite strip with a finite slit to a plane with two slits on the real axis, e.g., by

$$z = - \log w \ ,$$

where $z = x + iy$ and $w = u + iv$ are the complex variables in the physical and mapped planes, respectively. Then the mapping of these slits to concentric circles can be expressed in terms of the Elliptic Integral (see Kober[12])

$$\frac{\sigma}{r} = \exp \left\{ \int_{\infty}^{\zeta} \frac{ds}{\sqrt{4s(s-1)(s-e_2)}} \right\} \ ,$$

where e_2 is the value of u at the image of the profile trailing edge in the w plane, and $\bar{r}$ is the radius of the inner circle of the ring. The profile would be mapped to a nearly circular contour near the outer circle by this sequence of transformations. This contour could be mapped conformally to an exact circle by an iterative scheme similar to that used to map an isolated profile to a circle, or else a simple shearing transformation could be used to make it a coordinate line.

CONCLUSION

Some ideas for handling complex three-dimensional geometries in the finite-difference calculation of inviscid transonic flow patterns have been presented. An attractive approach seems to be to use nearly conformal maps in a family of coordinate surfaces which reduce the boundaries to those of the computational grid. A convenient mapping for use in calculations involving wing-fuselage combinations, fans, or three-dimensional cascades has been introduced, and sample results demonstrating its success in two-dimensional problems have been presented. Possible conformal mappings for the two-dimensional cascade (or wind tunnel) problem are also briefly discussed. These ideas have already proven effective in the calculation of transonic flows past swept and yawed wings. On the basis of these successes, we may expect the further application of these ideas to result in solutions with adequate accuracy for a variety of important engineering problems.

Finally, it should be noted that three-dimensional calculations require a substantial amount of computer time. For example, the swept wing calculation of Figure 1 requires about 75 minutes on the CDC 6600 (or 15-20 minutes on the CDC 7600). There are, however, a number of promising possibilities for accelerating the rates of convergence of the iterative schemes. For example, extrapolated relaxation[7], alternating direction methods[13], fast elliptic-solvers used in conjunction with relaxation[7,14], and a multi-grid method[15] have all been successfully applied to transonic problems. Thus, there appears to be the prospect of substantial reductions in the cost of these calculations.

REFERENCES

1. E. M. Murman and J. D. Cole, "Calculation of Plane, Steady, Transonic Flows," AIAA J., 9, 114, (1971).

2. W. F. Ballhaus and F. R. Bailey, "Numerical Calculation of Transonic Flow about Swept Wings," AIAA Paper 72-677, Presented at AIAA 5th Fluid and Plasma Dynamics Conference, Boston, Mass., June 26-28, 1972.

3. F. R. Bailey and W. F. Ballhaus, "Relaxation Methods for Transonic Flow about Wing-Cylinder Combinations and Lifting Swept Wings," Presented at Third International Conference on Numerical Methods in Fluid Dynamics, Paris, France, July 3-7, 1972.

4. P. R. Garabedian and D. G. Korn, "Analysis of Transonic Airfoils," Comm. Pure Appl. Math., 24, 841, (1972).

5. Antony Jameson, "Transonic Flow Calculations for Airfoils and Bodies of Revolution," Grumman Aerodynamics Report 370-71-1, December 1971.

6. J. C. South, Jr. and Antony Jameson, "Relaxation Solutions for Inviscid Axisymmetric Transonic Flow Over Blunt or Pointed Bodies," Proceedings of AIAA Computational Fluid Dynamics Conference, pp. 8-17, July 1973.

7. D. A. Caughey and Antony Jameson, "Accelerated Iterative Calculation of Transonic Nacelle Flowfields," AIAA Paper 76-100, Presented at AIAA 14th Aerospace Sciences Meeting, Washington, D. C. Jan. 26-28, 1976.

8. B. G. Arlinger, "Calculation of Transonic Flow Around Axisymmetric Inlets," AIAA Paper 75-80, presented at AIAA 13th Aerospace Sciences Meeting, Pasadena, California, Jan. 20-22, 1975.

9. Antony Jameson, "Iterative Solution of Transonic Flows over Airfoils and Wings, Including Flows at Mach 1," Comm. Pure Appl. Math. 27, 283, (1974).

10. Antony Jameson and D. A. Caughey, "Numerical Calculation of the Transonic Flow Past a Swept Wing," to appear.

11. M. H. Vavra, Aero-Thermodynamics and Flow in Turbomachinery, John Wiley and Sons, 1960.

12. H. Kober, Dictionary of Conformal Representations, Dover, 1957.

13. Antony Jameson, "An Alternating-Direction Method for the Solution of the Transonic Small-Disturbance Equation," New York University ERDA Report COO-3077-96.

14. Antony Jameson, "Accelerated Iterative Schemes for Transonic Flow Calculations using Fast Poisson-Solvers," New York University ERDA Report COO-3077-82.

15. Jerry C. South, Jr. and Achi Brandt, "Application of a Multi-Level Grid Method to Transonic Flow Calculations," Project SQUID Workshop on Transonic Flow Problems in Turbomachinery, Monterey, California, February 1976.

Figure Captions

Figure 1 (a) Geometry of Swept Wing.

Figure 1 (b) Upper and Lower Surface Pressure Distributions on Swept Wing.

Figure 2 Geometry of Wing-Fuselage Combination.

Figure 3 Normalized Geometry of Wing-Fuselage Combination.

Figure 4 Surface of r = constant, $(1 < r < r_{tip})$.

Figure 5 Nearly-Conformal Mapping of r = constant Surfaces.

Figure 6 Sketch of Boundaries in Computational Domain.

Figure 7 Geometry of an N-Bladed Fan.

Figure 8 Representative Mesh Distribution in Physical Plane (32 x 8 Grid).

Figure 9 (a) Pressure Distribution on Korn Airfoil in a Wind Tunnel, $h/c = 6.0$.

Figure 9 (b) Pressure Distribution on Korn Airfoil in a Wind Tunnel, $h/c = 4.0$.

Figure 10 A Mapping for Two-Dimensional Cascade Calculations.

Figure 1 (a) Geometry of Swept Wing.

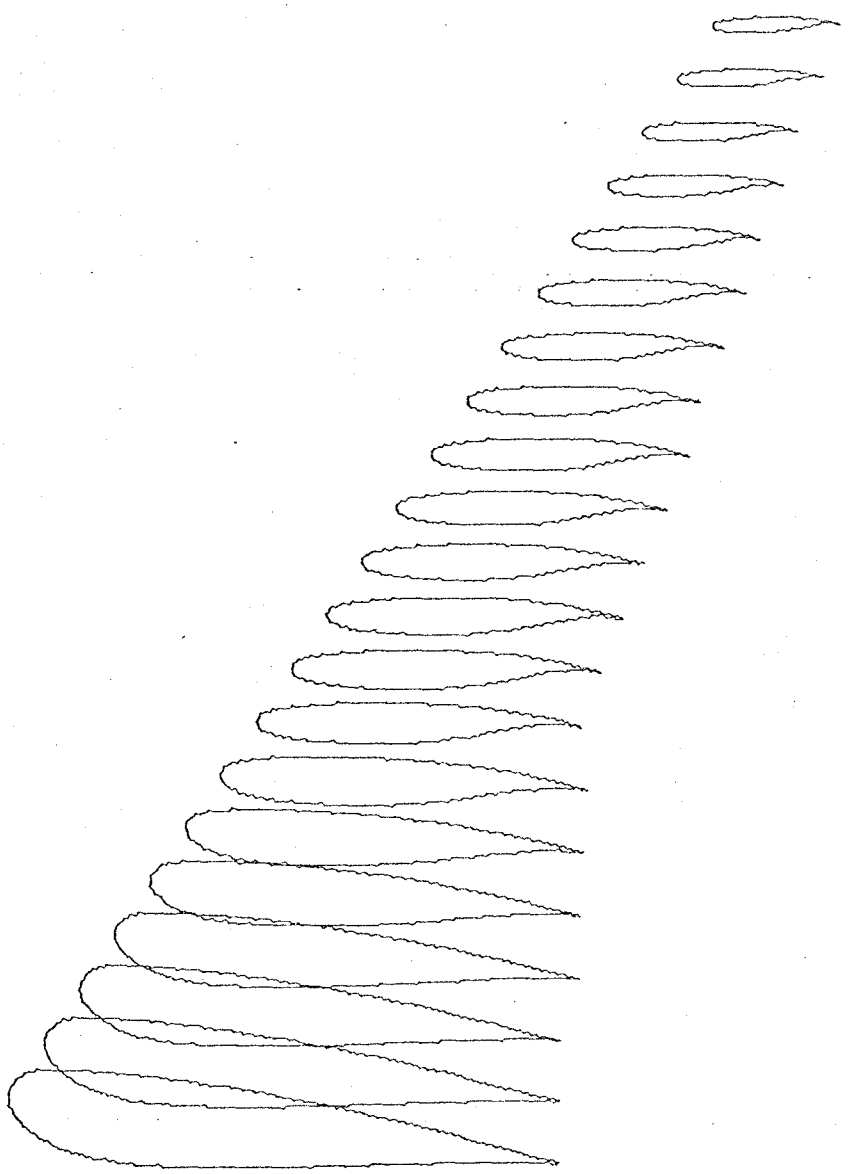

VIEW ØF WING

DØUGLAS WING W2 (EXTENDED TØ CENTER LINE)
M = .819 YAW = 0.00 ALF = 0.00
L/D = 26.68 CL = .5643 CD = .0211

Figure 1 (b) Upper and Lower Surface Pressure Distributions on Swept Wing.

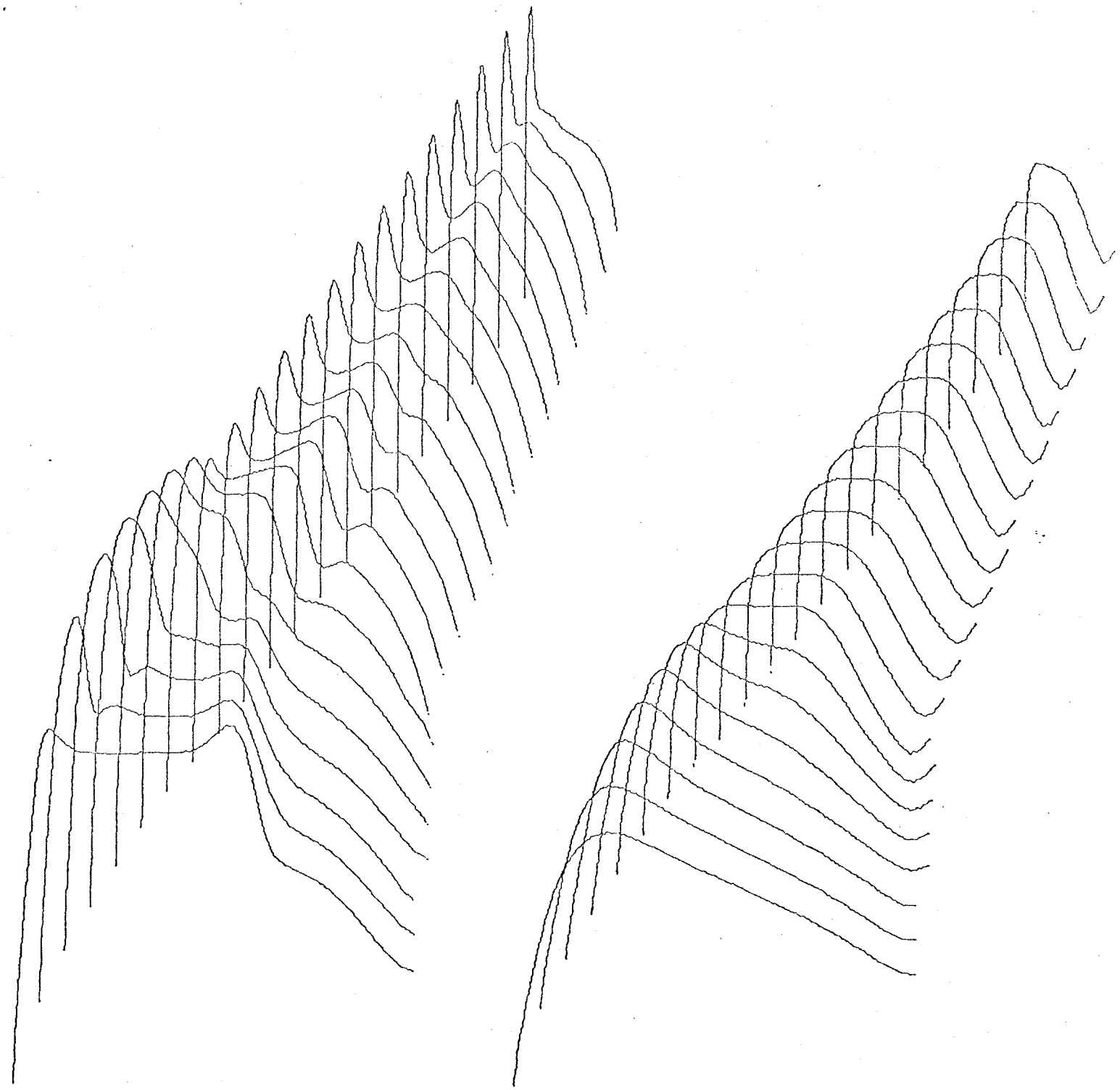

UPPER SURFACE PRESSURE LOWER SURFACE PRESSURE

DOUGLAS WING W2 (EXTENDED TO CENTER LINE)
M = .819 YAW = 0.00 ALF = 0.00
L/D = 26.68 CL = .5643 CD = .0211

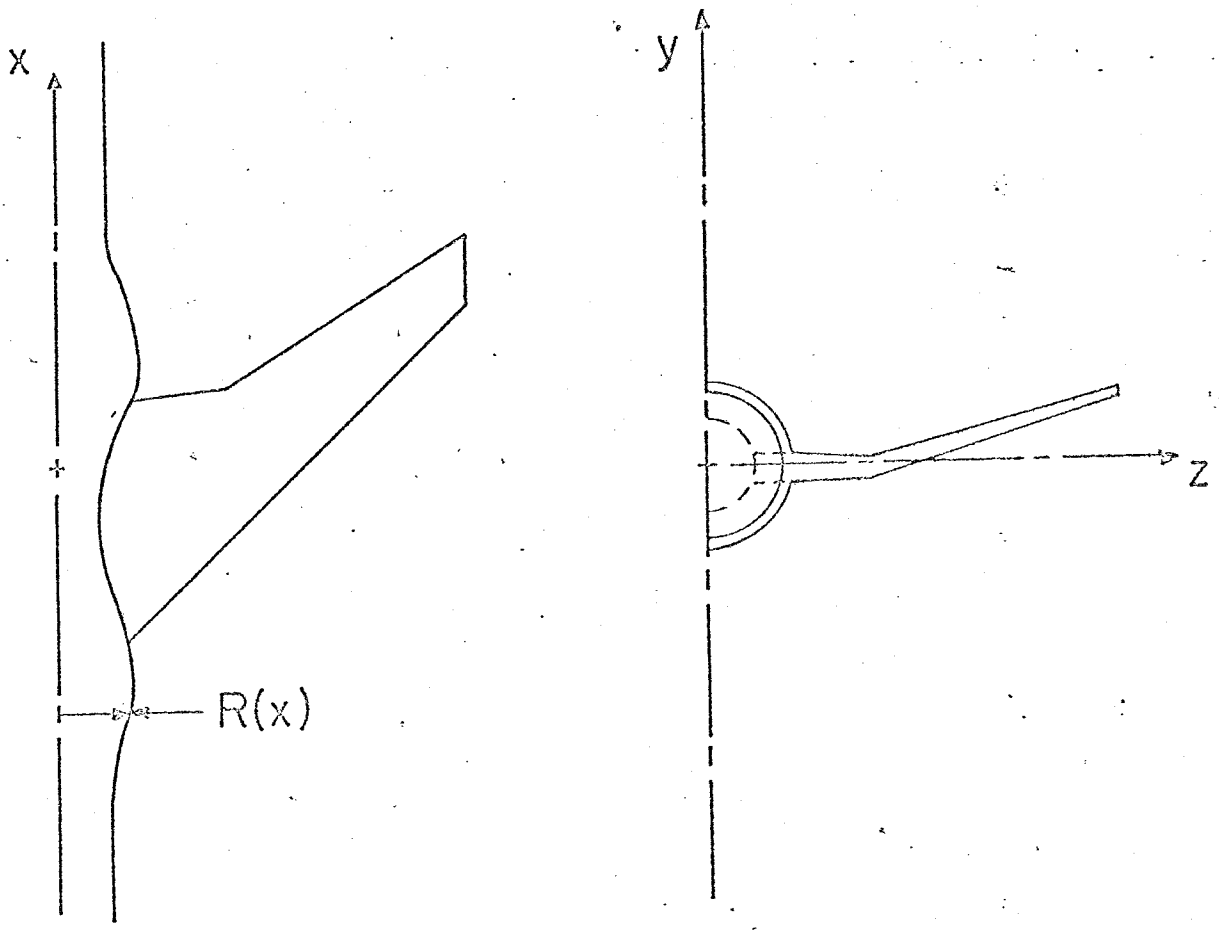

Figure 2 Geometry of Wing-Fuselage Combination.

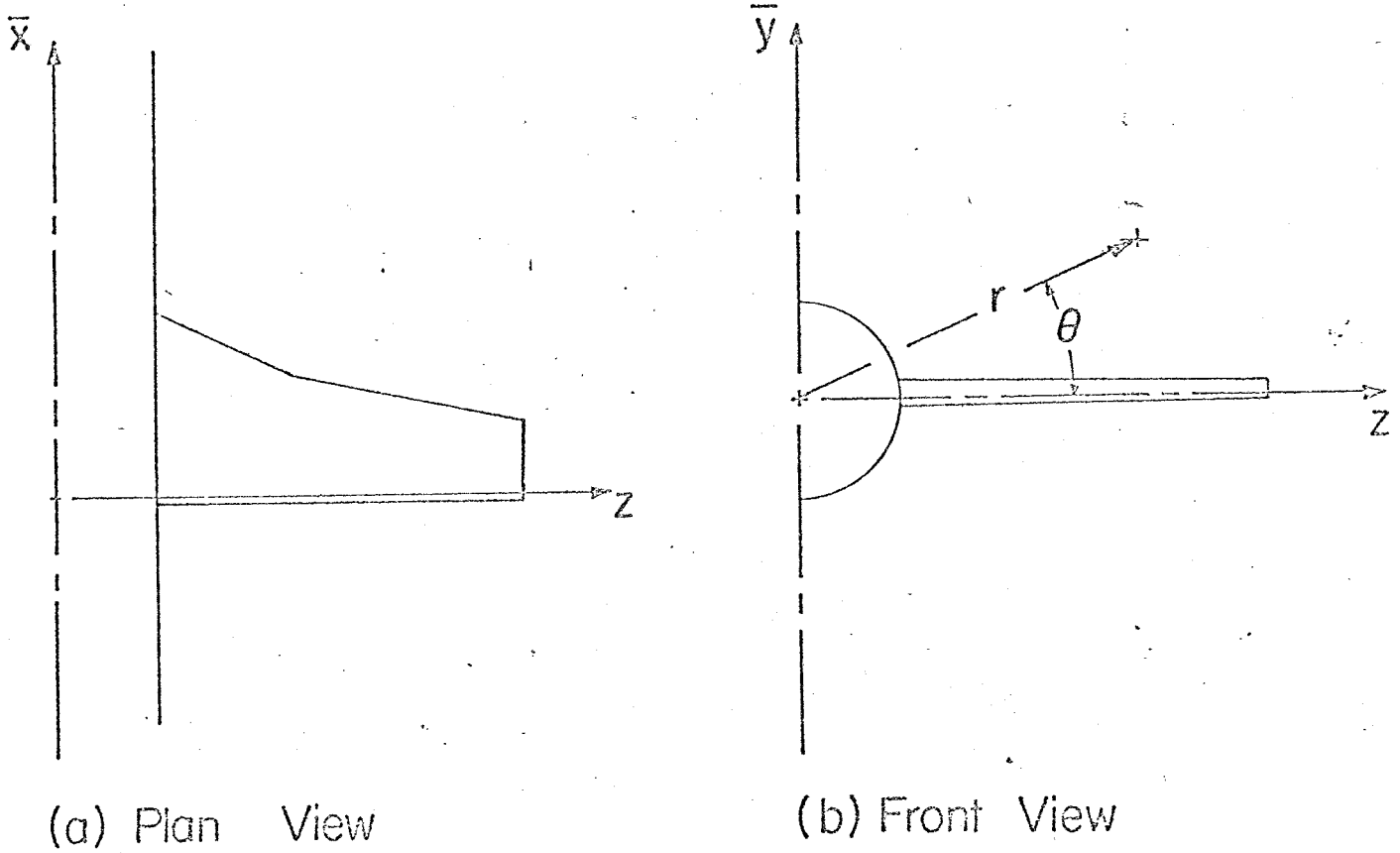

(a) Plan View

(b) Front View

Figure 3 Normalized Geometry of Wing-Fuselage Combination.

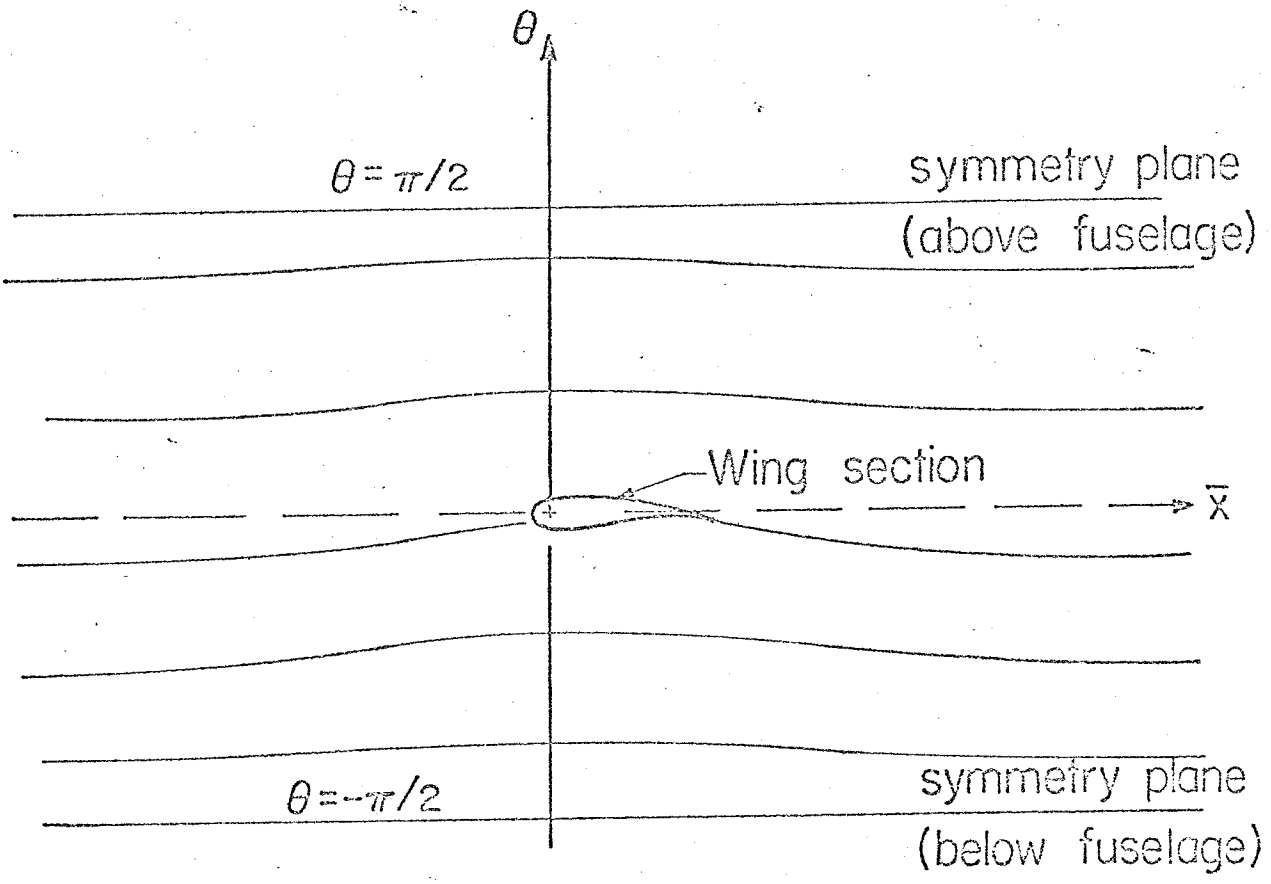

Figure 4 Surface of r = constant ($1. < r < r_{tip}$).

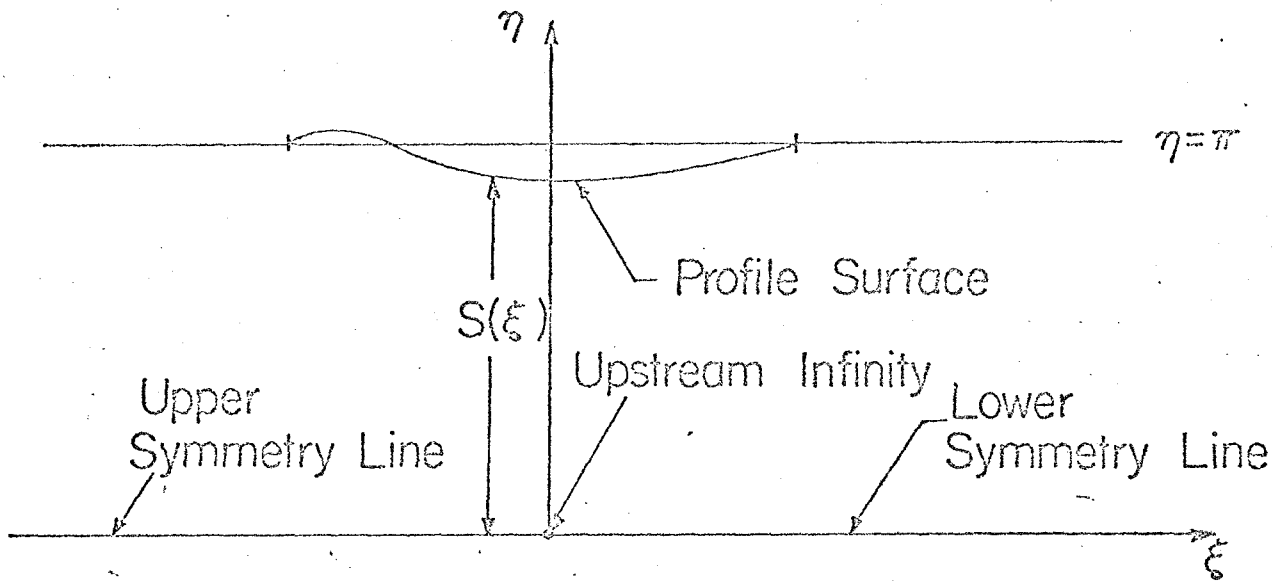

(a) Conformally-mapped plane

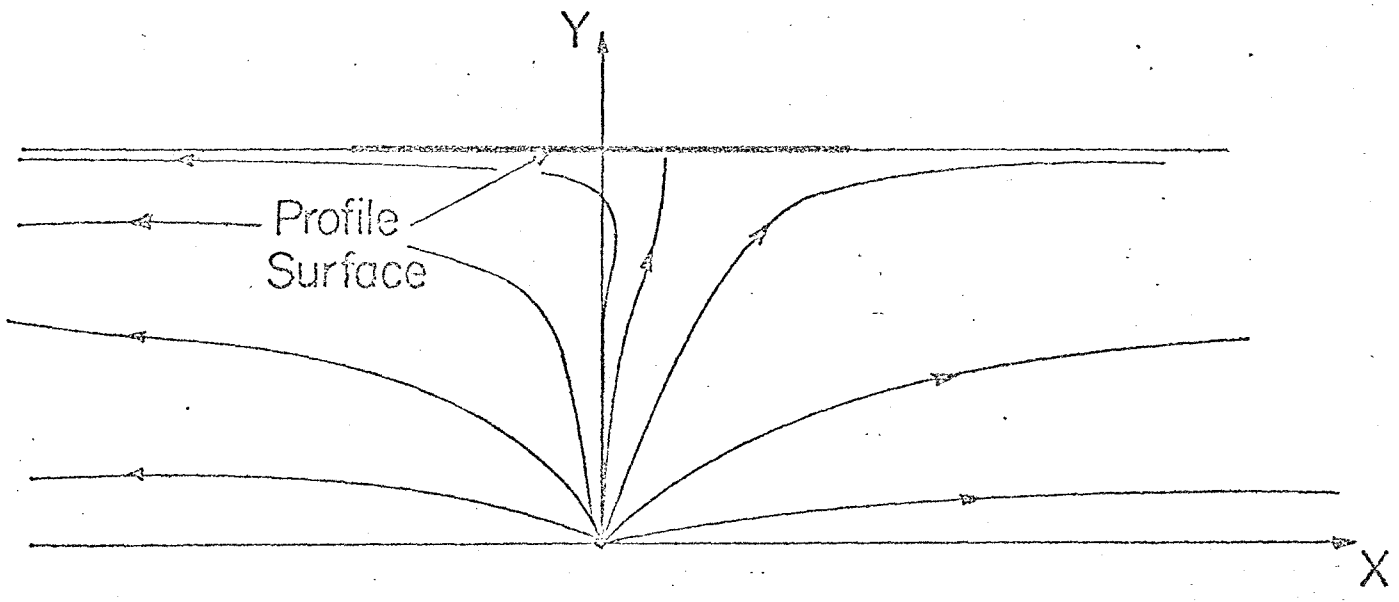

(b) Computational Plane (after shearing), showing schematic streamlines.

Figure 5 Nearly-Conformal Mapping of r = constant Surfaces.

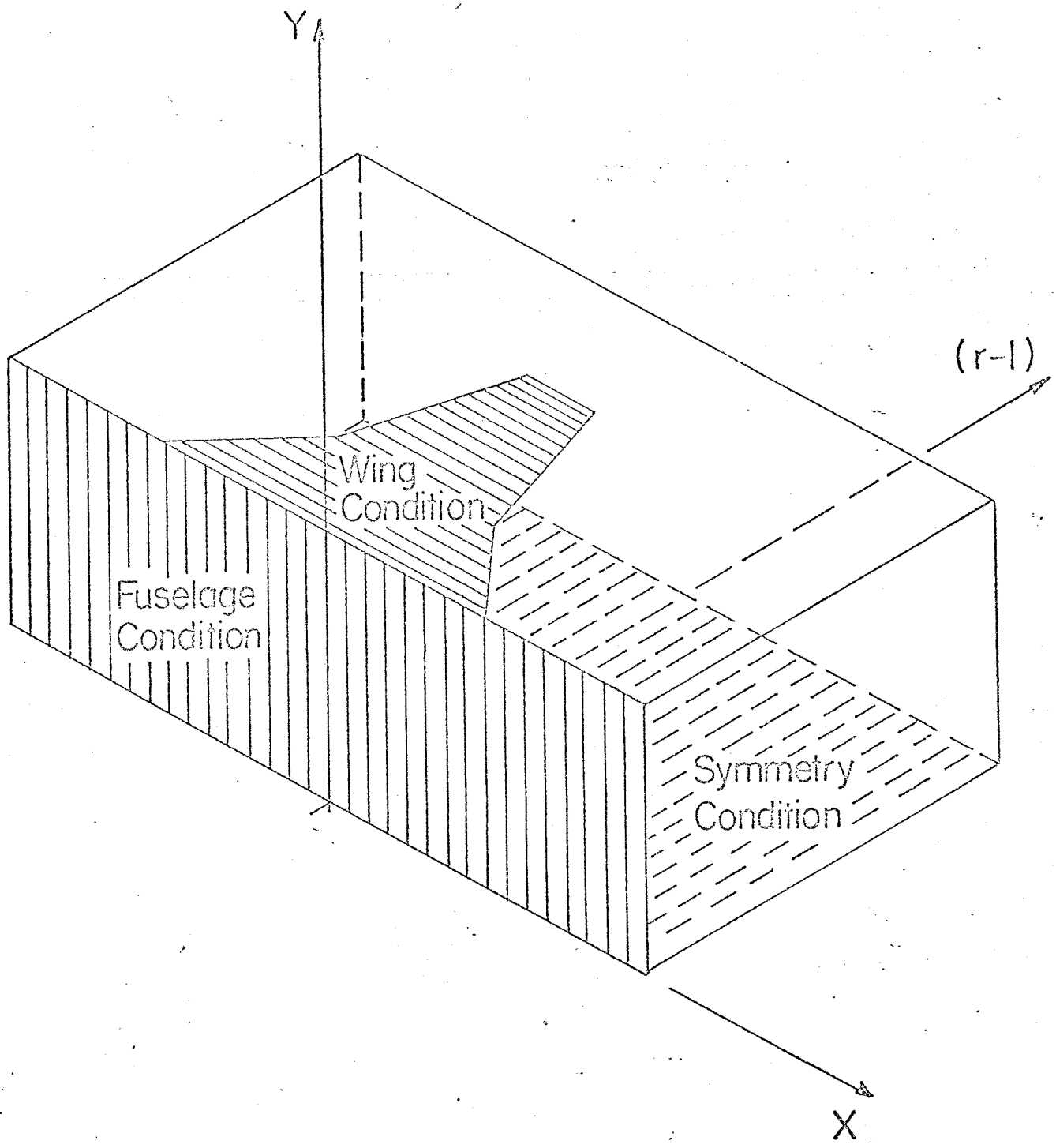

Figure 6 Sketch of Boundaries in Computational Domain.

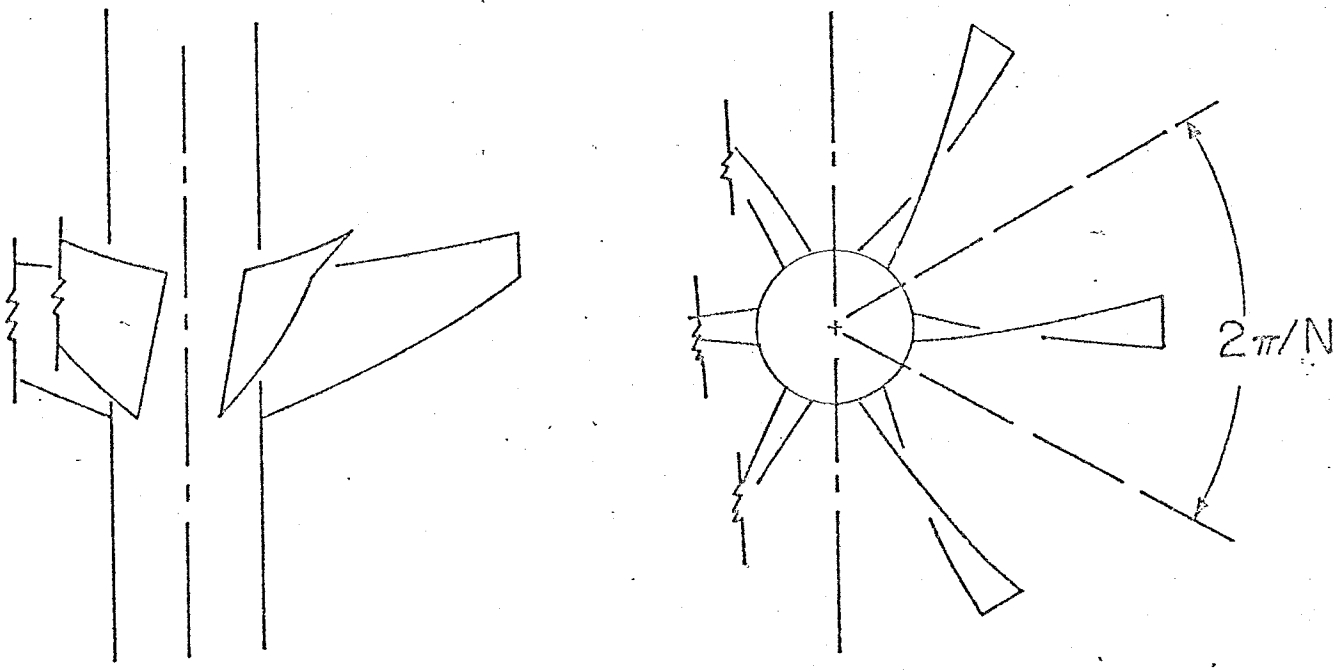

Figure 7 Geometry of an N-bladed Fan.

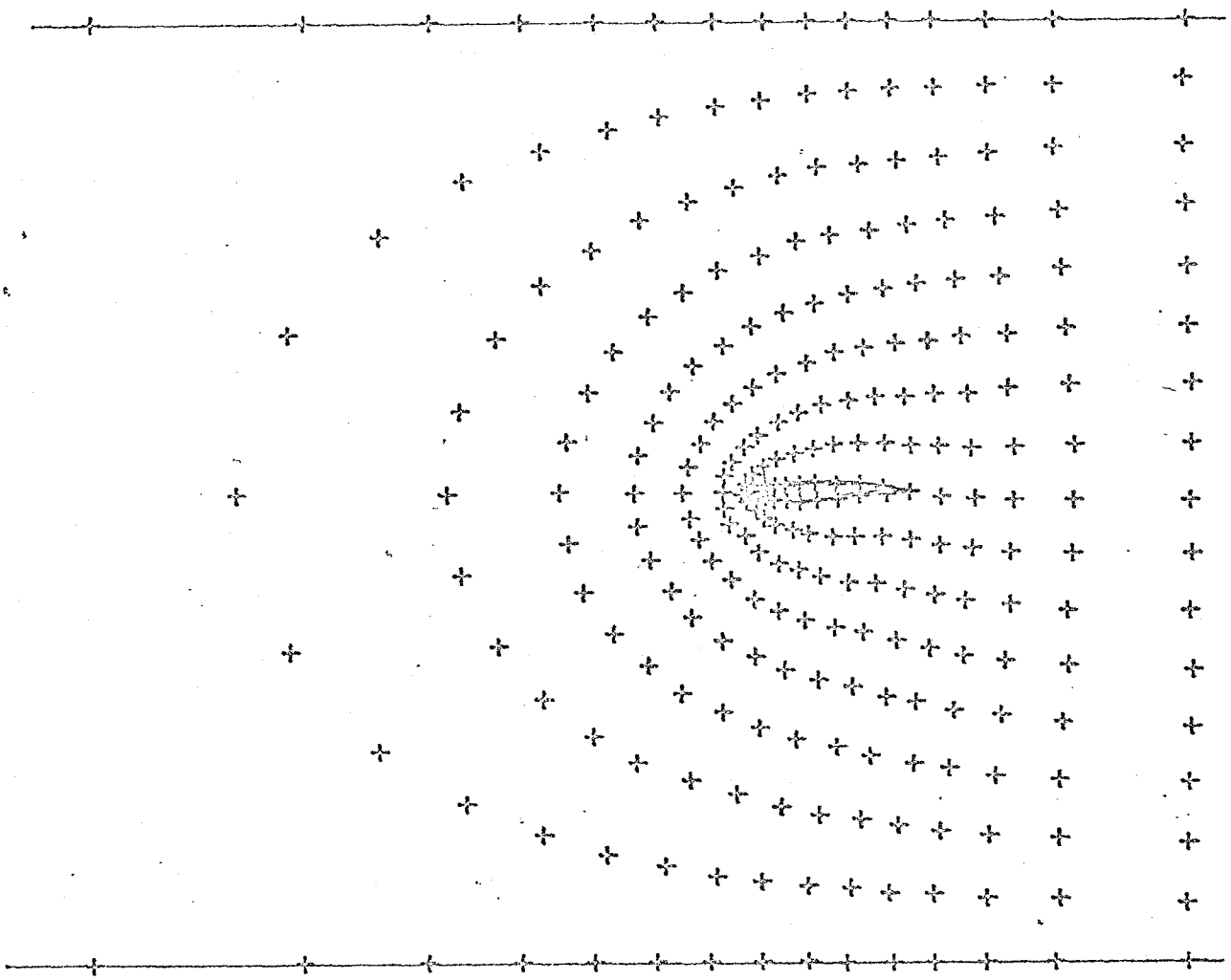

Figure 8 Representative Mesh Distribution in Physical Plane (32 x 8 Grid).

Figure 9 (a) Pressure Distribution on Korn Airfoil in a Wind Tunnel, h/c = 6.0.

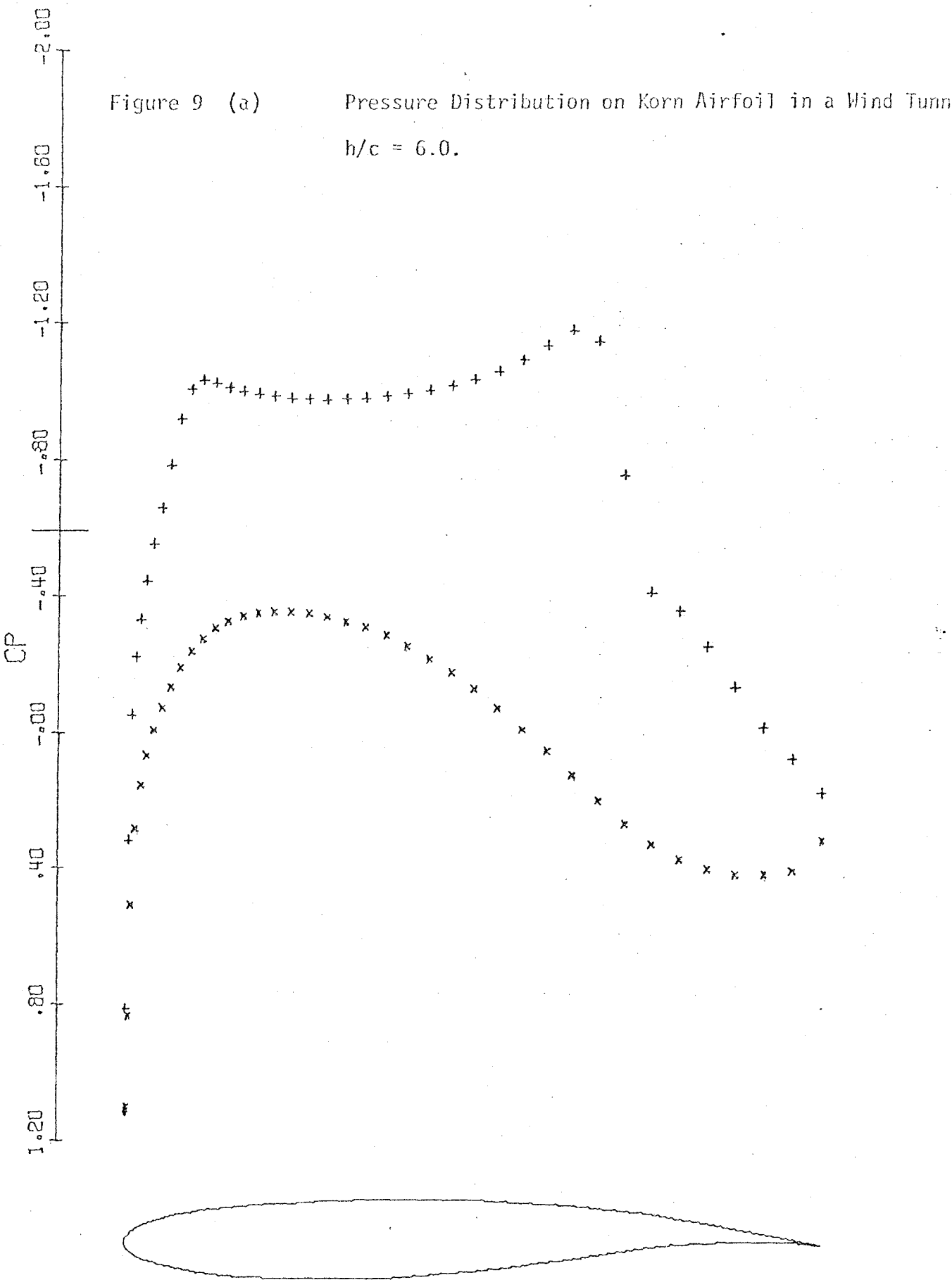

KØRN SHØCKFREE AIRFØIL

MACH	.750	ALPHA	0.000	HTC	6.000
CL	.7547	CD	.0069	CM	-.1888

Figure 9 (b) Pressure Distribution on Korn Airfoil in a Wind Tunnel, h/c = 4.0.

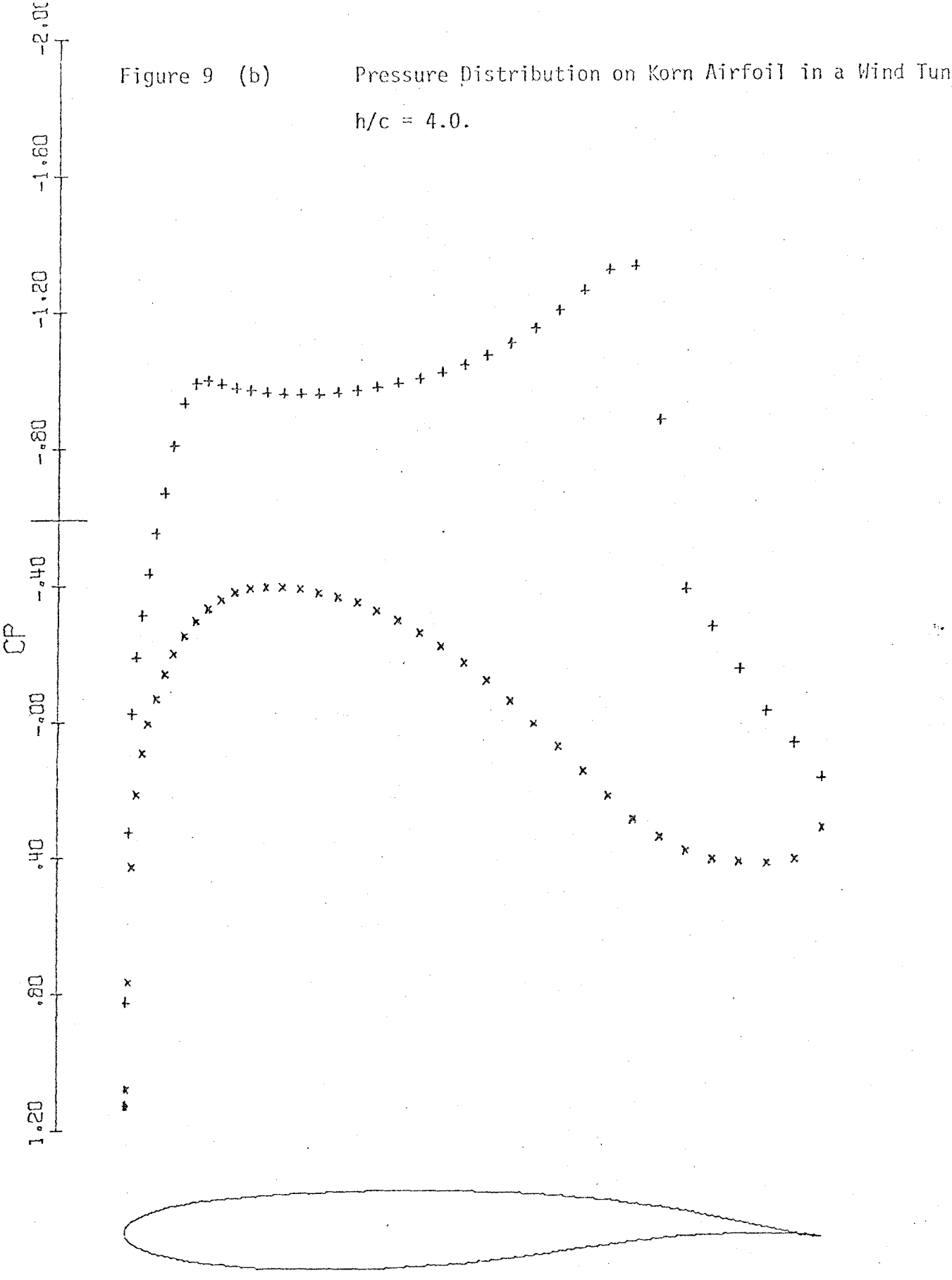

KØRN SHØCKFREE AIRFØIL

MACH	.750	ALPHA	0.000	HTC	4.000
CL	.7980	CD	.0177	CM	-.2235

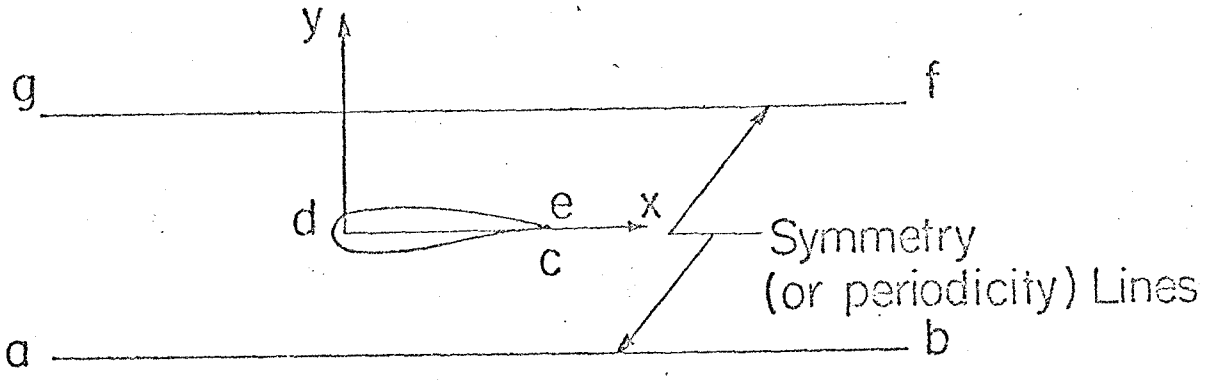

(a) Physical Plane (z-plane)

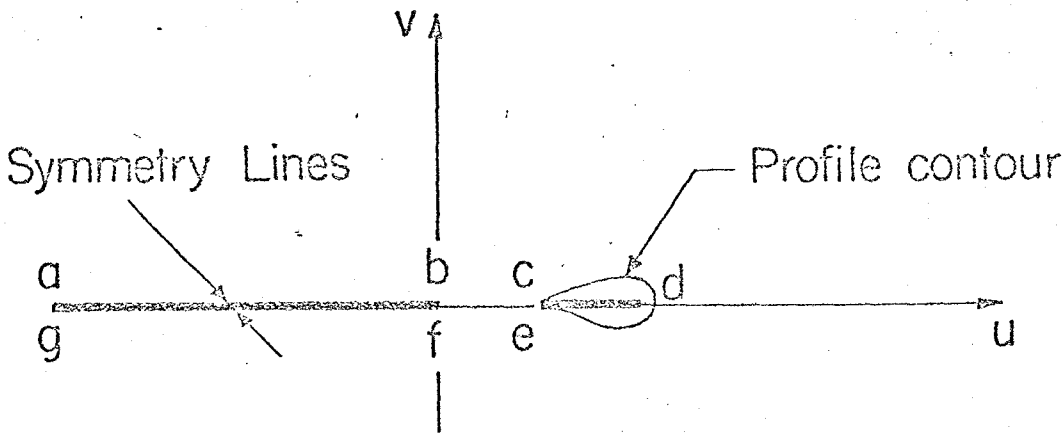

(b) Intermediate Plane with Two Slits (w-plane)

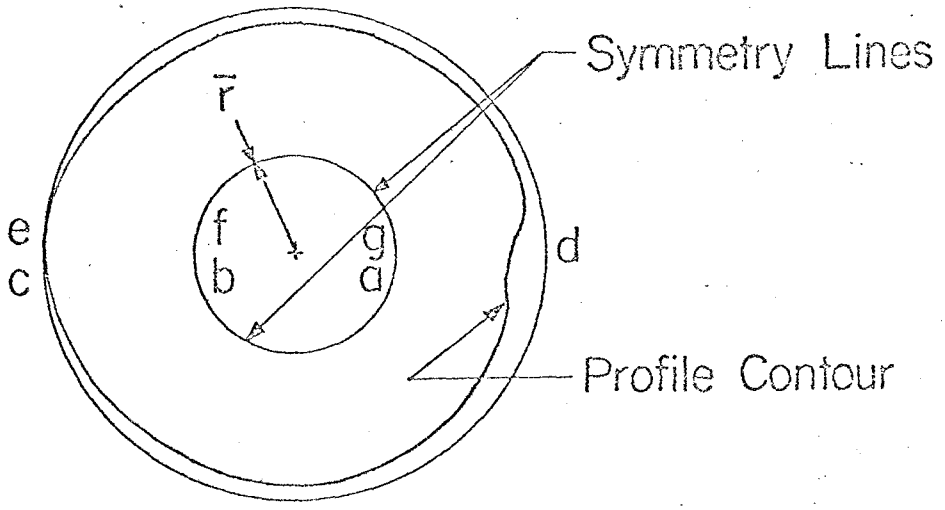

(c) Computational Ring (σ-plane)

Figure 10 A Mapping for Two-Dimensional Cascade Calculations.